John von Neumann Institute for Computing

Black Holes in Galactic Nuclei

Christoph Eichhorn, Patrick Glaschke,
and Rainer Spurzem

published in

NIC Symposium 2006 ,
G. Münster, D. Wolf, M. Kremer (Editors),
John von Neumann Institute for Computing, Jülich,
NIC Series, Vol. **32**, ISBN 3-00-017351-X, pp. 47-54, 2006.

http://www.fz-juelich.de/nic-series/volume32

Black Holes in Galactic Nuclei

Christoph Eichhorn[1,2]**, Patrick Glaschke**[1]**, and Rainer Spurzem**[1]

[1] Astronomisches Rechen-Institut, Zentrum Astronomie Univ. Heidelberg
Mönchhofstr. 12-14, 69120 Heidelberg, Germany

[2] Institut für Raumfahrtsysteme, Univ. Stuttgart
Pfaffenwaldring 31, 70550 Stuttgart, Germany

This project studies the formation, growth, and co-evolution of single and multiple massive black holes (MBHs) and compact objects like neutron stars, white dwarfs, and stellar mass black holes in galactic nuclei and star clusters, focusing on the role of stellar dynamics. In this paper we focus on one exemplary topic out of a wider range of work done, the study of orbital parameters of binary black holes in galactic nuclei (mass, spin, eccentricity, orbit orientation) as a function of initial parameters. In some cases the classical evolution of black hole binaries in dense stellar systems drives them to surprisingly high eccentricities, which is very exciting for the emission of gravitational waves and relativistic orbit shrinkage. Such results are interesting to the emerging field of gravitational wave astronomy, in relation to a number of ground and space based instruments designed to measure gravitational waves from astrophysical sources (VIRGO, Geo600, LIGO, LISA).

1 Introduction

MBH formation and their interactions with their host galactic nuclei is an important ingredient for our understanding of galaxy formation and evolution in a cosmological context, e.g. for predictions of cosmic star formation histories or of MBH demographics (to predict events which emit gravitational waves). If galaxies merge in the course of their evolution, there should be either many binary or even multiple black holes, or we have to find out what happens to black hole multiples in galactic nuclei, e.g. whether they come close enough together to merge under emission of gravitational waves, or whether they eject each other in gravitational slingshot. For numerical simulations of the problem all models depend on an unknown scaling behaviour, because the simulated particle number is not yet realistic due to limited computing power (Milosavljevic & Merritt 2001, 2003, Makino & Funato 2004, Berczik, Merritt & Spurzem 2005). Dynamical modelling of non-spherical dense stellar systems (with and without central BH) is even less developed than in the spherical case. Here we present a set of numerical models of the formation and evolution of binary black holes in rotating galactic nuclei. Since we are interested in the dynamical evolution of MBH binaries in their final phases of evolution (the last parsec problem) we somehow abstract from the foregoing complex dynamics of galactic mergers. We assume that after some violent dynamic relaxation a typical initial situation consists of a spherical or axisymmetric coherent stellar system (galactic nucleus), where fluctuations in density and potential due to the galaxy merger have decayed, which is reasonable on an (astrophysically) short time scale of a few ten million years. The MBHs, which were situated in the centre of each of the previously merged galaxies, are located at the boundary of the dense stellar core, some few hundred parsec apart. This situation is well observable
(e.g. Komossa et al. 2003).

According to the standard theory, the subsequent evolution of the black holes is divided in three intergradient stages (Begelman, Blandford & Rees 1980): 1. Dynamical friction causes an transfer of the black holes' kinetic energy to the surrounding field stars, the black holes spiral to the center where they form a binary. 2. While hardening, the effect of dynamical friction reduces and the evolution is dominated by superelastic scattering processes, that is the interaction with field stars closely encountering or intersecting the binaries' orbit, thereby increasing the binding energy. 3. Finally the black holes coalesce through the emission of gravitational radiation.

In this paper, the behavior of the orbital elements of a black hole binary in a dense stellar system is investigated. The evolution of the eccentricity has been discussed for some time (Makino et al. 1993, Hemsendorf, Sigurdsson & Spurzem 2002, Milosavljevic & Merritt 2001, Berczik, Merritt & Spurzem 2005, Makino & Funato 2005). According to Peters & Mathews (1963) and Peters (1964) the timescale of coalescence due to the emission of gravitational radiation is given by

$$t_{gr} = \frac{5}{64} \frac{c^5 a_{gr}^4}{G^3 M_1 M_2 (M_1 + M_2) F(e)} \tag{1}$$

wherein M_1, M_2 denote the black hole masses, a_{gr} the characteristic separation for gravitational wave emission, G the gravitational constant, c the speed of light and

$$F(e) = (1 - e^2)^{-7/2} \left(1 + \frac{73}{24} e^2 + \frac{37}{96} e^4 \right) \tag{2}$$

a function with strong dependence on the eccentricity e. Thus the coalescence time can shrink by several orders of magnitude if the eccentricity is high enough, resulting in a strengthened burst of gravitational radiation. Highly eccentric black hole binaries would represent appropriate candidates for forthcoming verification of gravitational radiation through the planned mission of the Laser Interferometer Space Antenna mission LISA.

The evolution of the semi-major axis can be consulted to characterize the hardening process of the binary. The behavior of the inclination is potentially interesting to predict processes related to angular momentum exchange between the black holes and the field stars, and in particular to strengthen the hypothesis of of the connection between the appearance of so-called X-shaped galaxies and supermassive black hole mergers in galactic nuclei (Merritt 2002, Zier & Biermann 2002).

2 Numerical Method, Initial Models

The simulations have been performed using NBODY6++, a parallelized version of Aarseth's NBODY6 (Aarseth 1999, Spurzem 1999, Aarseth 2003). The code includes a Hermite integration scheme, KS-regularization (Kustaanheimo & Stiefel 1965) and the Ahmad-Cohen neighbour scheme (Ahmad & Cohen 1973). No softening of the interaction potential of any two bodies is introduced; this allows an accurate treatment of the effects due to superelastic scattering events, which play a crucial part in black hole binary evolution and require a precise calculation of the trajectories throughout the interaction. The code and its parallel performance has been described in detail in this series and elsewhere (Spurzem 1999, Khalisi et al. 2003). The survey has been carried out for a total particle number $N = 64\,000$ including two massive black holes with $M_1 = M_2 = 0.01$ embedded

in a dense stellar system of 63998 equal-mass particles $m_* = 1.5625 \cdot 10^{-5}$. The total mass of the system is normalized to unity.

The initial stellar distribution was taken from generalized King models with rotation (Lagoute & Longaretti 1996, Longaretti & Lagoute 1996, Einsel & Spurzem 1999). Main parameters are the dimensionless central potential W_0, describing the degree of central concentration, and the dimensionless rotation parameter ω_0. We have performed a series of models for $W_0 = 0, 3, 6$, $\omega_0 = 0.0, 0.3, 0.6$ (the last value means that there is a 20% fraction of rotational kinetic energy in the system, which is still a mild flattening); furthermore we have varied the initial velocity of the MBHs to be v_c, $\sqrt{2}v_c$, and $0.136v_c$, where v_c is the tangential velocity of a circular orbit at the initial MBH position. Other parameters of the problem, which we have not yet varied extensively, are the mass ratio of the black holes to the stars and the mass ratio of the black holes to each other.

3 Simulations

3.1 Evolution of the Binding Energy

We measure the relative two-body energy, angular momentum and other orbital elements of the MBH binary from the beginning of our simulations. In the first evolutionary stage, each black hole individually suffers from dynamical friction with the surrounding low mass stars, which is the main process of losing energy. Note that for simplicity we also use the above defined energy (and also the eccentricity definition e of a bound two-body orbit) even if the MBH binary is not yet bound. In such a case E and e are just numerical values which give informations about the relative state of motion of the two MBHs, but do not imply that they are already bound.

The role of dynamical friction decreases when a permanently bound state occurs, as the dynamical friction force acts preferentially on the motion of the now formed binary rather than on the individual black holes. Superelastic scattering events of field stars at the binary shall be more and more important for the reduction of its energy. These events cause a stochastic variation of E and e in our models. Nevertheless energy and angular momentum (which determined e) undergo a diffusive process with a net change of orbital parameters on top of the stochastic variations. In the stage when superelastic scattering dominates the picture, the energy loss rate is commonly written in terms of the dimensionless hardening constant H

$$\frac{d}{dt}\left(\frac{1}{a}\right) = HG\frac{\rho}{\sigma} \tag{3}$$

where a is the separation of the black holes, ρ the mass density and σ the velocity dispersion in the environment of the binary (see e.g. Merritt 2001). In other words, the process leads to a continous hardening of the MBH binary, provided there are always enough interaction partners available (the "loss cone is full", see discussions in Milosavljevic & Merritt 2003, Berczik, Merritt & Spurzem 2005).

Our measured hardening constants are in majority slightly below the $H = 8.4$ published elsewhere (Hemsendorf, Sigurdsson & Spurzem 2002), where a Plummer model was used, however. The lower values can be possibly explained by the fact that dynamical friction might still have a noticeable influence. Regarding our calculated a_h as criteria for

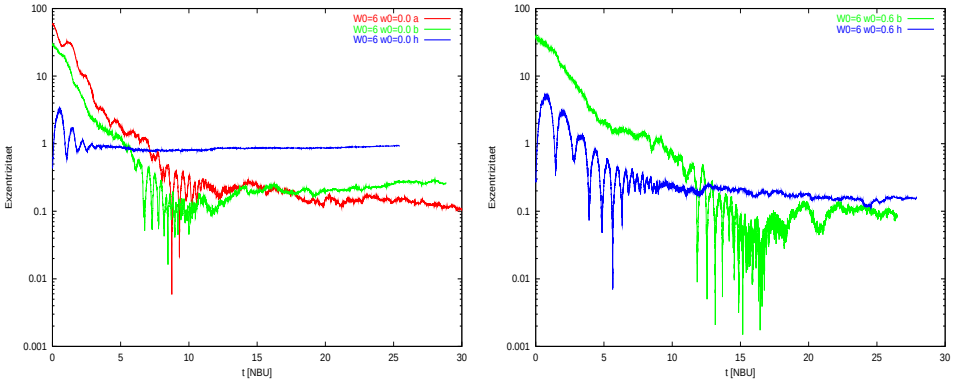

Figure 1. Time evolution of the MBH eccentricity. King parameter $W_0 = 6$; $\omega_0 = 0.0$ *left*, no rotation, $\omega_0 = 0.6$ *right*, rotation. Different initial velocities are indicated with different colours, $v_0 = 0.136 v_c$ *blue*, $v_0 = v_c$ *green*, and $v_0 = \sqrt{2} v_c$ *red*.

the domination of superelastic scattering events, the hardening separation could be significantly smaller if σ increases during the simulation as $a_h \propto \sigma^{-2}$. An enhanced σ can be expected for ρ/σ =const. if it is assumed that the black hole would capture stars during the simulation and raise the central density.

3.2 Eccentricity

The eccentricity is given by

$$e = \sqrt{1 + \frac{2El^2}{\mu (G M_1 M_2)^2}} \tag{4}$$

where M_i ($i = 1, 2$) are the masses of the two black holes, $\mu = M_1 M_2/(M_1 + M_2)$ is the reduced mass, G the gravitational constant, E the energy, and l the specific angular momentum of the two black holes relative to each other. Fig.1 shows some results for the calculated eccentricity evolution. Each plot assorts simulations of a fixed pair of King parameters under variation of the initial velocity.

Obviously, simulations with an initial velocity comparable to the circular velocity tend to end up in low-eccentricity motions of the black hole components, while $v_0 = 0.136 v_c$ runs reach generally higher final eccentricities. This behavior was already indicated by Makino et al. (1993), who simulated two black holes of the masses $M = 0.01$ im a Plummer sphere of 16348 particles. They found very high final eccentricities $e \sim 0.99$ applying very low initial velocities, while their largest value, $v_0 = 0.5 v_c$, reached a noticeably smaller final $e \sim 0.665$.

The dependency of the final eccentricity on initial velocities can be understood by considering the black hole trajectories. In Fig. 2, for $v_0 = v_c$, the black holes spiral at first independently of each other to the center. The influence of dynamical friction causes a steady loss of kinetic energy. Within the time interval $t = [10.11; 20.14]$, the total energy becomes negative and the binary reaches a bound state; in the following the binary hardens, the separation decreases due to superelastic scattering events and the circular motion center

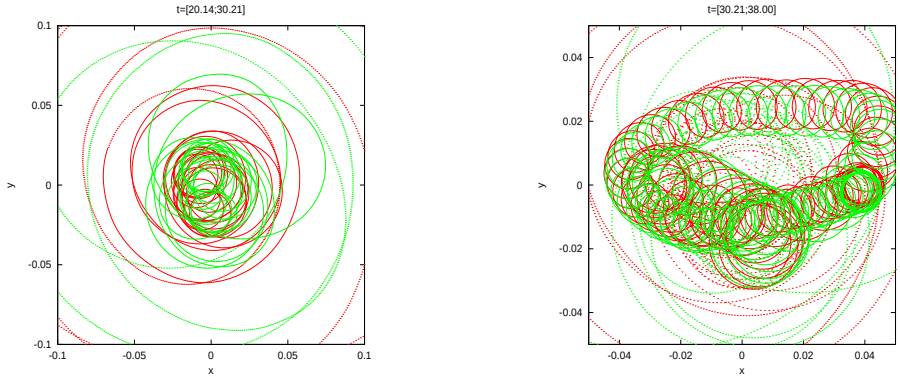

Figure 2. Trajectories for the model $W_0 = 3$, $\omega_0 = 0.3$, $v_0 = v_c$ in the projection on the xy-plane. Red and green mark the orbit of a black hole respectively. Solid lines indicate the trajectories passed through in the time interval mentioned above each figure, the dotted lines hint the orbit before. Note the scaling of the axes in different figures.

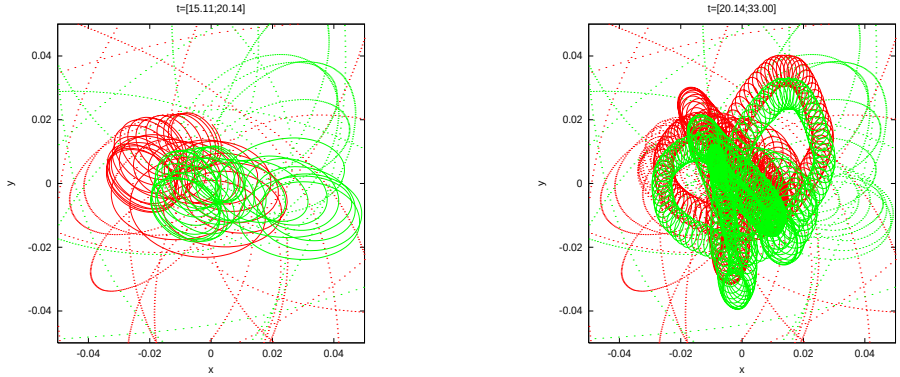

Figure 3. the same as in Fig.2, but with $v_0 = 0.136 v_c$

of mass of the binary itself becomes visible. At the time the attractive force between the black holes becomes comparable to the gravitational force of the stellar distribution, the individual trajectories of the black holes are still circular around the systems center of mass. This means that the circular orbits generated by the initial velocity is ”conserved” until the binary reaches a bound state and beyond as dynamical friction is not strong enough to change the trajectories dramatically.

A different situation arises for $v_0 = 0.136$. As a consequence of the low velocity, the black holes must plunge near to the center, but dynamical friction is at the time of the closest encounter (the pericenter of the relative motion) not sufficiently effective to prevent the re-swing to the outer regions and to circularize the orbits in this way. Therefore, the initial form of the orbits is kept until the end of the simulation. We have studied a much wider parameter range than described here and also looked at other orbital elements of the

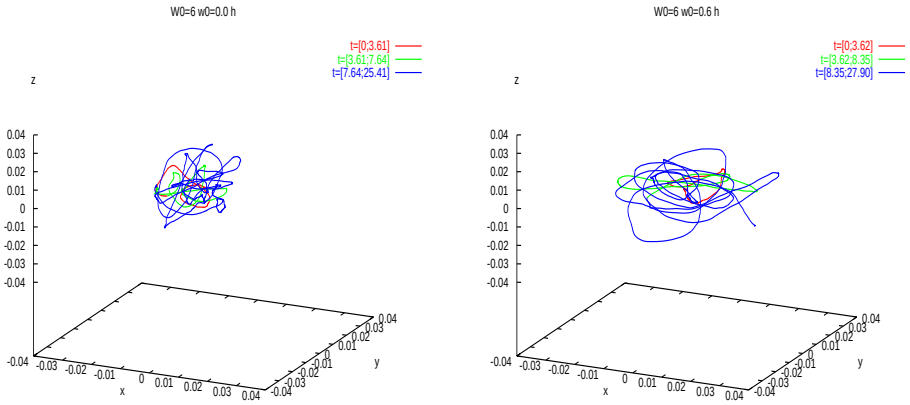

Figure 4. Three-dimensional diagram of the centre-of-mass trajectories of our MBH, $W_0 = 6$ and $v_0 = 0.136 v_c$. The rotation parameters are $\omega_0 = 0.0$ *left* and $\omega_0 = 0.6$ *right*. The different colours indicate the orbits in the denoted time intervals respectively.

MBH (e.g. its inclination relative to the galactic plane, which could be an observable due to the large scale radio jets emitted from the central MBH engines in galactic nuclei), and we have also studied the effect of co- and counterrotation (different angular momentum axis of the stellar system and the initial MBH motion). The interested reader will find a complete review of our results in Eichhorn & Spurzem (2006, MNRAS, in preparation).

3.3 Brownian Motion

The center of mass (CM) of a hardened binary is expected to to perform an irregular motion in the central region of the stellar system. This motion is often described by the concept of Brownian motion, as it is characterized by a friction force (dynamical friction) and a fluctuating force (as the result of scattering events and encounters of field stars). We have measured and analysed the Brownian motion of an MBH due to superelastic scatterings in detail, but show here only one exemplary picture as a typical result.

We conclude from this section: (1) The final eccentricity is strongly dependent on the initial black hole velocities. (2) The eccentricity is dependent on the rotation parameter of the model. (3) Determined hardening rates agree within the expected systematic and statistical error with previously published work. (4) Only weak changes in the inclination and in the orientation of the angular momentum vector direction have been observed, consistent with simulations by Milosavljevic & Merritt (2001). (5) Counter rotation simulations yield noticeably different results in eccentricity, in one case actually an extreme large value $\bar{e} = 0.997$. (6) Brownian motion of the center of mass of the binary is influenced by the rotation of the stellar system (points (4) to (6) are just given here but not discussed in further detail).

4 Computational and Algorithmic Issues

We use a timing model for our parallel code which is flexible and usable for many different kinds of hardware. It is

$$T = \alpha\Big(\frac{N^2}{n_p} + \frac{NN_n}{n_p} + A\ln_2 n_p + BN\Big) \tag{5}$$

where T is the total wall clock time, the four summands (from left to right) are the regular and irregular (neighbour) force computation time, latency and bandwidth dominated communication time (note that a new communication scheme is assumed here, which reduces the latency, which is not yet included in all our simulations. In the old case the latency scaled linearly with n_p). N, N_n, n_p are the total particle number, the neighbour number in the Ahmad-Cohen neighbour scheme, and n_p the processor number used. α, A, B are a time and two dimensionless constants depending on the hardware. Measurements on the IBM Jump deliver values of $\alpha \approx 0.3\mu$ sec, $A \approx 500$, $B \approx 2$, with fluctuations of a factor of 2 to 3 depending on details of the simulation. With these new data we can derive a new value for the optimal neighbour number, which is $N_{n,\mathrm{opt}} \propto N^{3/5}$ for small N (up to about 10^4) and $N_{n,\mathrm{opt}} \propto N^{1/5}$ for larger N. This is significantly smaller than the previously proposed value of Makino & Hut (1988), $N_{n,\mathrm{opt}} \propto N^{3/4}$. With a smaller neighbour number less communication is required and thus larger processor numbers can be used. Our algorithm always works best if we have a balance between communication and computation (this work and more details will be found in Glaschke, 2006, Ph.D. thesis in preparation, and be published elsewhere, too).

Note also, that despite a very good efficiency of our code the use of special purpose hardware such as GRAPE is more efficient for the largest particle numbers (such as 10^5 or 10^6). Recent supercomputers which combine standard CPUs with application acceleration processors (e.g. CRAY XD1 with FPGA chips) offer a promising path to join both advantages (A. Ernst, ongoing work in progress).

5 Outlook, Other Subprojects

In ongoing studies we are right now transcending the limits of Newtonian dynamics. At the termination of the simulations shown above, in particular the very high e-cases, relativistic corrections cause measurable (in the sense of the accuracy of the numerical model) changes in the orbital elements. We have included these terms as perturbative forces in the KS regularisation up to the so-called Post-Newtonian order 2.5, which includes two orders of perihel shifts and the lowest dissipative term, sufficient to describe gravitational radiation (Kupi, Amaro-Seoane & Spurzem 2005, in preparation). In future work more relativistic effects could be included, such as spin-spin and spin-orbit couplings, and linear momentum recoil at MBH binary coalescence. A collaboration with G. Schäfer and G. Achamveedu (Jena) is being developed to properly formulate these terms. Scaling requires that one cannot simulate such systems without realistic particle number. Such models are proposed in the DEISA scheme.

6 Acknowledgements

Computing time at NIC Jülich on the IBM Jump is acknowledged. Financial support comes partly from Volkswagenstiftung, SFB439 at the University of Heidelberg and the Studienstiftung des Deutschen Volkes (P.G.). It is always a pleasure to acknowledge Sverre Aarseth, without his help and continuous support over many years this work would not be possible.

References

1. Aarseth S.J., 1999a, Publ. Astr. Soc. Pac. 111, 1333.
2. Aarseth, S., 2003, *Gravitational N-body simulations* (Cambridge University Press, Cambridge), p.173.
3. Ahmad A., Cohen L., Journal of Computational Physics 1973, 12, 349.
4. Begelman M.C., Blandford R.D., Rees M.J., 1980, Nature, 287, 307.
5. Berczik, P., Merritt, D., Spurzem, R. 2005, ApJ, in press (astro-ph/0507260).
6. Einsel C., Spurzem R., 1999, 1999, MNRAS, 302, 81.
7. Hemsendorf M., Sigurdsson S., Spurzem R., 2002, ApJ, 581, 1256.
8. Khalisi, E., Omarov, C.T., Spurzem, R., Giersz, M., Lin, D.N.C. 2003, in "High Performance Computing in Science and Engineering", Springer Vlg., pp. 71-89.
9. Komossa S., Burwitz V., Hasinger G., Predehl P., Kaastra J.S., Ikebe, Y., 2003, ApJ, 582, L15.
10. Kustaanheimo P., Stiefel E., Journal für die reine und angewandte Mathematik 1965, 218, 204.
11. Lagoute C., Longaretti P.-Y., 1996, A&A, 308, 441.
12. Longaretti P.-Y., Lagoute C., 1996, A&A, 308, 453.
13. Makino J., Fukushige T., Okumura S.K., Ebisuzaki T., 1993, PASJ 45, 303.
14. Makino J. , Funato Y. 2004, ApJ, 602, 93.
15. Merritt D., 2001, ApJ, 565, 245.
16. Merritt, D., 2002, ApJ 568, 998.
17. Milosavljević M., Merritt D., 2001, ApJ, 563, 34.
18. Milosavljević M. , Merritt D. 2003, ApJ, 596, 860.
19. Peters P.C., 1964, Phys.Rev., 136, B1224.
20. Peters P.C., Mathews J. 1963, Phys. Rev. 131, 435.
21. Spurzem R., 1999, Journal of Computational and Applied Mathematics, 109, 407.
22. Zier C., Biermann P.L., 2002, A&A, 396, 91.